

## NATURAL CONFIGURATIONS AND CONTROLLED MOTIONS SUITABLE FOR FORMATION FLYING

**G. Gómez\***, **M. Marcote<sup>†</sup>**, **J.J. Masdemont<sup>‡</sup>**, and **J.M. Mondelo<sup>§</sup>**

Assume that a constellation of satellites is required to flight close a given nominal trajectory and that there is some freedom in the selection of the geometry of the constellation. If we are interested in avoiding large variations of the mutual distances between the spacecrafts, we can consider the possible existence of regions of zero relative radial acceleration with respect to the nominal trajectory. The motion along these regions will prevent from the expansion or contraction of the constellation. The goal of this paper is the study of these regions and the controlled motions between them.

### INTRODUCTION

The present paper is devoted to study natural configurations suitable for formation flying, as well as the controlled motions between these configurations. Most of the work is done in the force model defined by the Restricted Three Body Problem, although it can be easily extended to the general n–body problem, as is shown in the paper.

The concrete goals of the paper are:

- The study of geometries, around arbitrary nominal orbits of the n–body problem, with good properties for formation flight.
- The study of controlled motions between the zero relative radial acceleration cones obtained from the preceding analysis.

As reference solutions, along which we will assume that the formation is moving, we will use a libration point orbit of the Sun-Earth system and a transfer trajectory from the Earth (see Fig. 1). Nevertheless, this choice has been taken only for illustration purposes and, in principle, any kind of trajectory can be used.

---

\* IEEC & Departament de Matemàtica Aplicada i Anàlisi, Universitat de Barcelona, Gran Via 585, 08007 Barcelona, Spain. e-mail:gerard@maia.ub.es.

† Departament de Matemàtica Aplicada i Anàlisi, Universitat de Barcelona, Gran Via 585, 08007 Barcelona, Spain. e-mail:marcote@maia.ub.es.

‡ IEEC & Departament de Matemàtica Aplicada I, Universitat Politècnica de Catalunya, E.T.S.E.I.B., Diagonal 647, 08028 Barcelona, Spain. e-mail:josep@barquins.upc.edu.

§ IEEC & Departament de Matemàtiques, Universitat Autònoma de Barcelona, 08193 Bellaterra (Cerdanyola del Vallès) Barcelona, Spain. e-mail:jmm@mat.uab.es.

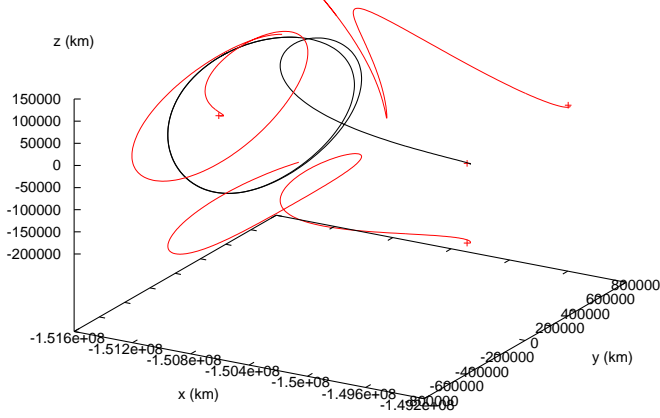


Figure 1: Halo orbit and transfer trajectory (of the stable manifold of the halo orbit) and coordinate projections. The points marked with a cross show the position of the Earth and its projections on the coordinate planes.

## THE ZERO RELATIVE RADIAL ACCELERATION CONES

In order to avoid expansion or contraction in a constellation of space-crafts, with the corresponding large variations of the mutual distances between them, we have studied the existence of regions with zero relative radial acceleration (ZRRA). For a simple model, such as the RTBP, it is possible to get an analytical expression for the above regions, provided the radius of the constellation (largest separation between the spacecrafts) is small, so that a linear approach to the problem gives the relevant information about the local dynamics of the problem.

We write the RTBP equations of motion as the first order system of differential equations (see [2])

$$\begin{aligned}
 \dot{x} &= \xi, \\
 \dot{y} &= \eta, \\
 \dot{z} &= \zeta, \\
 \dot{\xi} &= 2\eta + x - (x + \mu)\frac{1 - \mu}{r_1^3} - (x + \mu - 1)\frac{\mu}{r_2^3}, \\
 \dot{\eta} &= -2\xi + y \left( 1 - \frac{1 - \mu}{r_1^3} - \frac{\mu}{r_2^3} \right), \\
 \dot{\zeta} &= -z \left( \frac{1 - \mu}{r_1^3} + \frac{\mu}{r_2^3} \right),
 \end{aligned} \tag{1}$$

with  $r_1 = \sqrt{(x + \mu)^2 + y^2 + z^2}$ ,  $r_2 = \sqrt{(x + \mu - 1)^2 + y^2 + z^2}$ .

Denoting the above system by  $\dot{\mathbf{x}} = \mathbf{f}(\mathbf{x})$ , the linear behaviour around a solution  $\mathbf{x}(t)$  is

given by

$$\dot{\mathbf{u}} = D\mathbf{f}(\mathbf{x}(t))\mathbf{u}, \quad (2)$$

where

$$Df = \left( \begin{array}{ccc|ccc} 0 & 0 & 0 & 1 & 0 & 0 \\ 0 & 0 & 0 & 0 & 1 & 0 \\ 0 & 0 & 0 & 0 & 0 & 1 \\ \hline f_x^4 & f_y^4 & f_z^4 & 0 & 2 & 0 \\ f_x^5 & f_y^5 & f_z^5 & -2 & 0 & 0 \\ f_x^6 & f_y^6 & f_z^6 & 0 & 0 & 0 \end{array} \right) = \left( \begin{array}{c|c} 0 & I \\ \hline F & J \end{array} \right),$$

and  $f^4$ ,  $f^5$ ,  $f^6$  are the last three component of the vector-field  $\mathbf{f}$ , of which we have to compute their partial derivatives with respect to  $x$ ,  $y$  and  $z$  in order to get the symmetric sub-matrix  $F$ . Writing the array  $\mathbf{u}$  as  $(\mathbf{r}, \dot{\mathbf{r}})^T$ , the linear system (2) becomes

$$\begin{pmatrix} \dot{\mathbf{r}} \\ \ddot{\mathbf{r}} \end{pmatrix} = \begin{pmatrix} 0 & I \\ F & J \end{pmatrix} \begin{pmatrix} \mathbf{r} \\ \dot{\mathbf{r}} \end{pmatrix}. \quad (3)$$

The points with zero relative velocity are those such that  $\dot{\mathbf{r}} = 0$ , and, in this case, have that the relative acceleration is given by

$$\ddot{\mathbf{r}} = \dot{\mathbf{v}} = F\mathbf{r}.$$

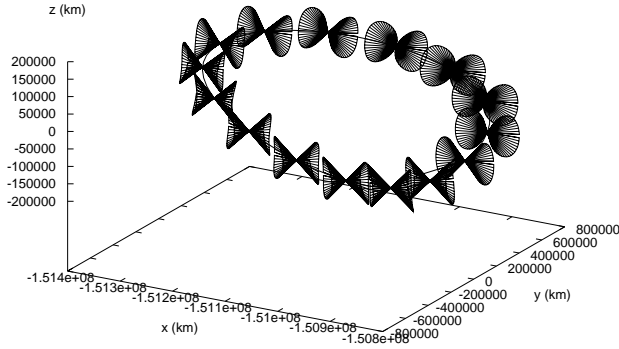


Figure 2: Zero relative radial acceleration cones along a halo orbit.

To get the radial component of the relative acceleration we must compute the scalar product of  $\ddot{\mathbf{r}}$  with  $\mathbf{r}$ . This radial component will be zero for the set of points such that

$$\mathbf{r}^T F \mathbf{r} = 0. \quad (4)$$

Equation (4) represents, in general, a quadric which depends on the point  $\mathbf{x}(t)$  selected along the nominal solution of (1). For the reference halo orbit displayed in Fig. 1, the zero relative radial acceleration cones (ZRRAC), at different points of the orbit, are shown in in Fig. 2.

The ZRRAC can be also computed numerically. Given a certain nominal trajectory, we selected a point on it  $(\mathbf{x}(t), \mathbf{v}(t))$ . Around this point we consider a sphere, in the configuration space, of radius equal to  $3 \cdot 10^{-9}$  adimensional RTBP units (0.5 km) and we set the velocity of all the points of the sphere equal to the velocity of the point selected,  $\mathbf{v}(t)$  (zero relative velocity condition). Parametrising the sphere by the longitude  $\lambda$  and the latitude  $\phi$ , the test points of the sphere will be of the form

$$(\mathbf{x}(t) + \mathbf{s}(\lambda, \phi), \mathbf{v}(t)).$$

Now, writing the equations of motion of the RTBP as

$$\ddot{\mathbf{x}} = \mathbf{g}(\mathbf{x}, \dot{\mathbf{x}}),$$

we can evaluate the relative acceleration by

$$\mathbf{a}(t; \lambda, \phi) = \mathbf{g}(\mathbf{x}(t), \mathbf{v}(t)) - \mathbf{g}(\mathbf{x}^h(t) + \mathbf{s}(\lambda, \phi), \mathbf{v}(t)),$$

whose scalar product with  $\mathbf{s}(\lambda, \phi)$  will give the desired relative radial acceleration. In Fig. 3 we show the behaviour of this function for different points along the transfer trajectory.

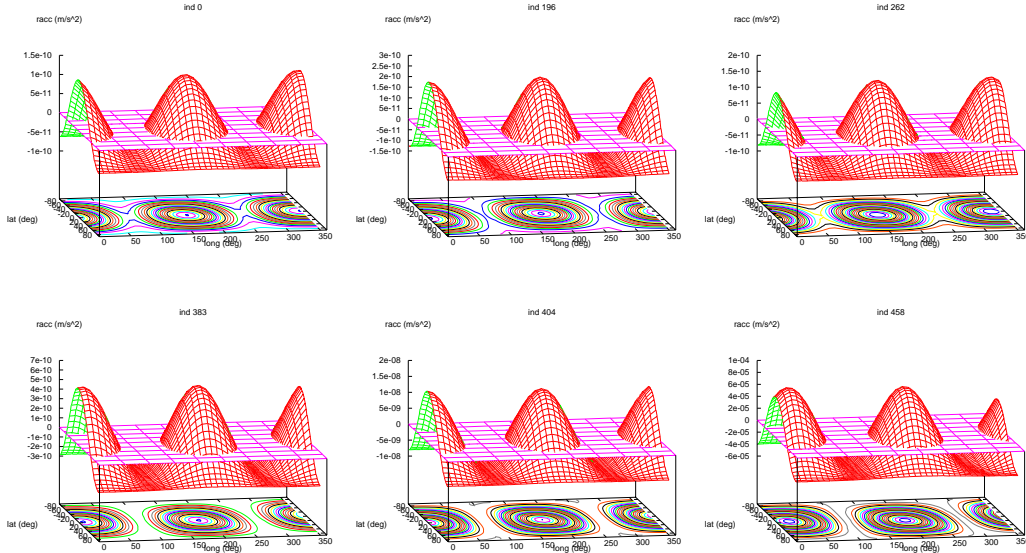


Figure 3: Relative radial velocity surfaces associated to the points along the transfer trajectory.

The qualitative behaviour of the function  $\mathbf{a}(t; \lambda, \phi)$  is almost the same for all the values of  $t$ , either if we move along the halo orbit or along the transfer trajectory. There appear two maxima, associated to the unstable directions, and two minima, related to the stable ones. The function  $\mathbf{a}$  is zero along two cones with vertex at  $\mathbf{x}(t)$ , these cones give the most suitable directions to set a constellation of spacecrafts. In principle, a set of aligned

spacecrafts placed on them will keep fixed their mutual distances. This relative behaviour will be shown later.

The cones of zero relative radial acceleration obtained with the analytical linear approach reproduce, qualitatively and quantitatively, the behaviour detected numerically. The numerical determination can be easily extended to more realistic models of motion, such as the JPL model, as is shown in Fig. 4.

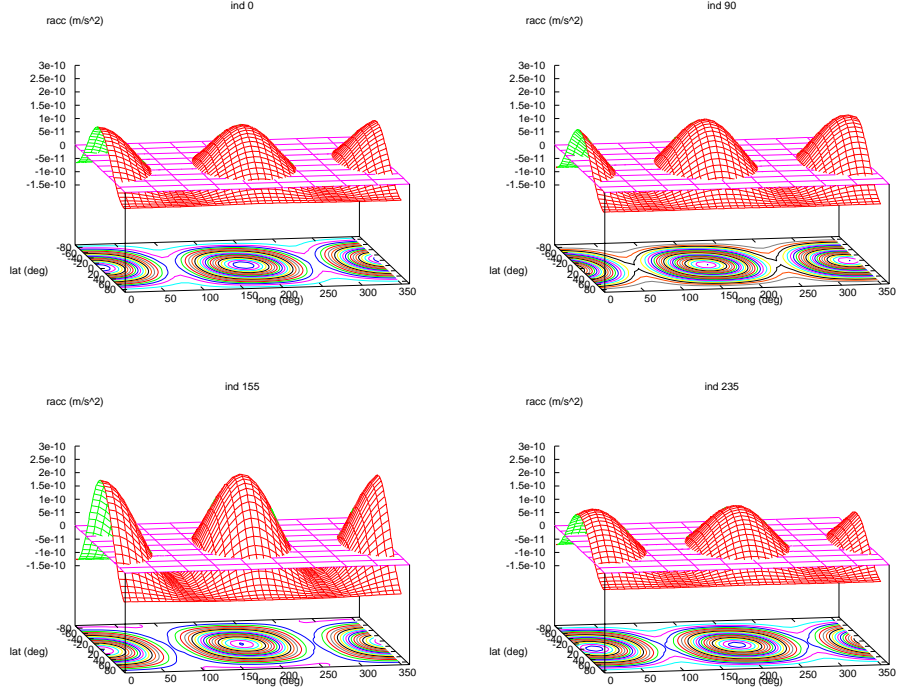


Figure 4: Relative radial velocity surfaces associated to four different points of the refined halo orbit in the full JPL model for the Solar System motion.

## DYNAMICAL BEHAVIOUR ALONG THE ZRRAC

In this section we show the dynamical behaviour of the different kinds of solutions with initial conditions along the most relevant directions determined in the preceding section.

For the first simulation, we have taken five points  $p_0, \dots, p_4$  along the direction of maximum radial acceleration associated to the initial condition of the halo orbit of the RTBP. We will denote this point by  $p_0$ . The points have been distributed symmetrically with respect to  $p_0$ :  $p_2, p_3$  being at a distance of 0.25 km from  $p_0$  and  $p_1, p_4$  at a distance of 0.5 km.

We have integrated these points for a full period of the periodic halo orbit (approximately 180 days) and the results are shown in Fig. 5. As it can be seen, even starting along the most expansive direction, the orbits do not deviate too much from the periodic orbit during

this time span. Nevertheless, the behaviour of the distance to the halo orbit,  $d(p_i(t), p_0(t))$ , is exponential, as it should be (Fig. 5 right). Also, there is no difference between the qualitative behaviour of  $d(p_i(t), p_0(t))$  for the trajectories starting at the same distance from  $p_0$ :  $d(p_2(t), p_0(t)) \approx d(p_3(t), p_0(t))$  and  $d(p_1(t), p_0(t)) \approx d(p_4(t), p_0(t))$ .

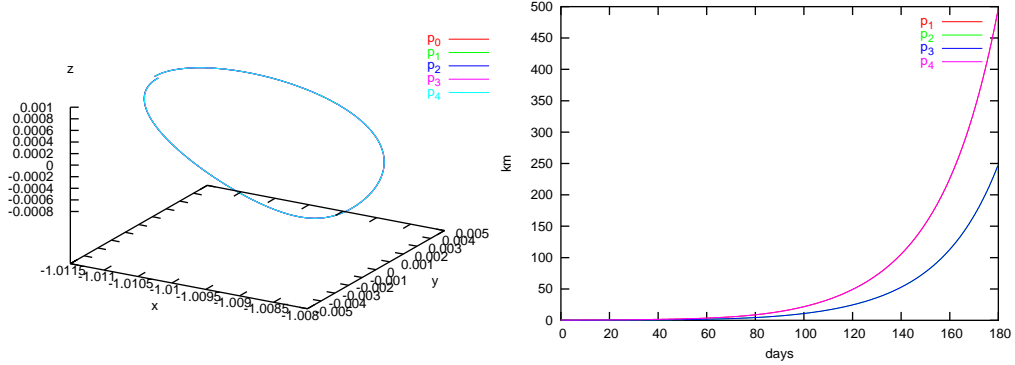


Figure 5: Left: trajectories followed by the points chosen along the direction of maximum relative radial acceleration. Right: distances,  $d(p_i(t), p_0(t))$ , between the trajectories of  $p_1, p_2, p_3, p_4$  and the base halo orbit  $p_0(t)$ .

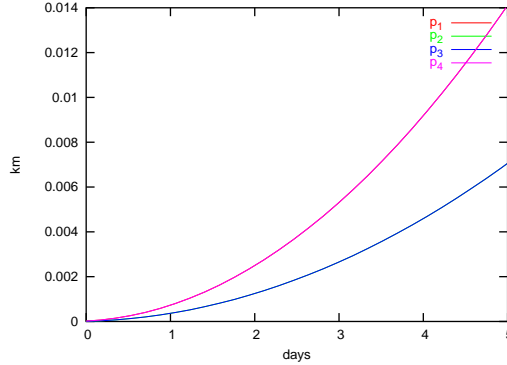


Figure 6: Values of the differences  $d(p_i(t), p_0(t)) - d(p_i(0), p_0(0))$  ( $d(p_i(0), p_0(0)) = 0.25$  km for  $i = 2, 3$  and  $0.50$  km for points  $i = 1, 4$ ) for a 5-day time span.

In Fig. 6 we have displayed the deviations of the actual positions with respect to the initial ones:  $d(p_i(t), p_0(t)) - d(p_i(0), p_0(0))$ . As it can be seen from this figure, after five days they are of the order of 14 meters. This corresponds to an acceleration of  $4.734 \times 10^{-3}$  (m/s)/yr, which is approximately equal to the maximum relative radial acceleration computed.

Now, let us test the opposite situation and start from four points along a generatrix of the zero relative radial acceleration cone, corresponding also to the initial condition of the halo orbit of the RTBP, distributed in a similar fashion to the previous case.

In Fig. 7 we show the results for the  $d(q_i(t), q_0(t))$  function, corresponding to the integration during a full period (180 days) of the different initial condition. Now, although the qualitative behaviour is still exponential, the final distances are shorter (they are reduced

by a factor of 3) than the ones obtained for the  $p_i$  points taken along the unstable direction.

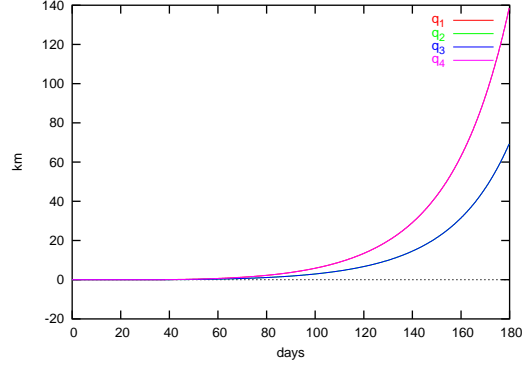


Figure 7: Distances,  $d(q_i(t), q_0(t))$ , between the trajectories of  $q_1, q_2, q_3, q_4$  and the base halo orbit  $q_0(t)$ .

In the left plot of Fig. 8 we display the results corresponding to an integration analogous to the one of Fig. 6. As it can be seen, the maximum deviation from the starting separations is now less than 50 *cm* while for the  $p_i$  points was of 14 *m*. In the right plot of the same figure, we represent the separations for a 50-day time-interval. The behaviour of the relative distance changes from being governed by radial accelerations around the base orbit to being governed by exponential escape inherent to the libration point orbit.

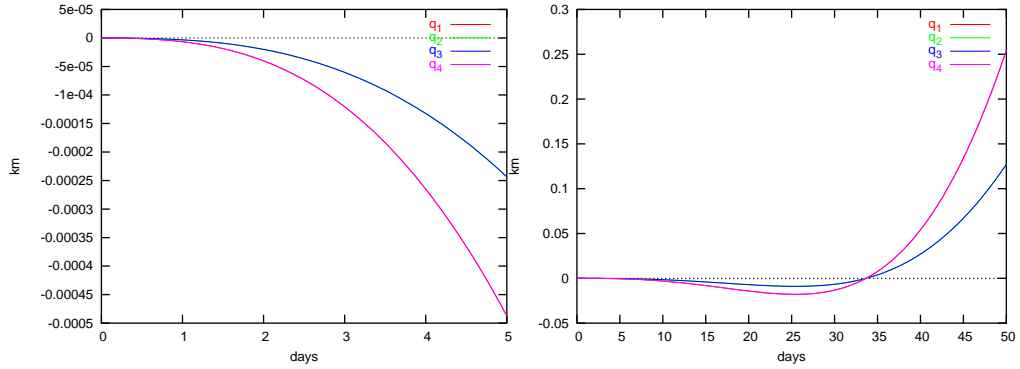


Figure 8: Deviations  $d(p_i(t), p_0(t)) - d(p_i(0), p_0(0))$  from the starting separations from the nominal orbit of the paths followed by the points  $q_1, q_2, q_3, q_4$ , for a 5-day time-interval (left) and for a 50-day one (right).

In order to show that the JPL model behaves in the same way as the RTBP does, we have performed the same two kinds of computations as before: taking initial conditions along the “worst” and “best” directions. using as initial epoch the 1/1/2000.

In Figs. 9 and 10 we have represented the deviation from the initial separation from the base orbit of the points  $p_i$  and  $q_i$  of the JPL model. It is seen that the behaviour is very similar to the one displayed for the RTBP model.

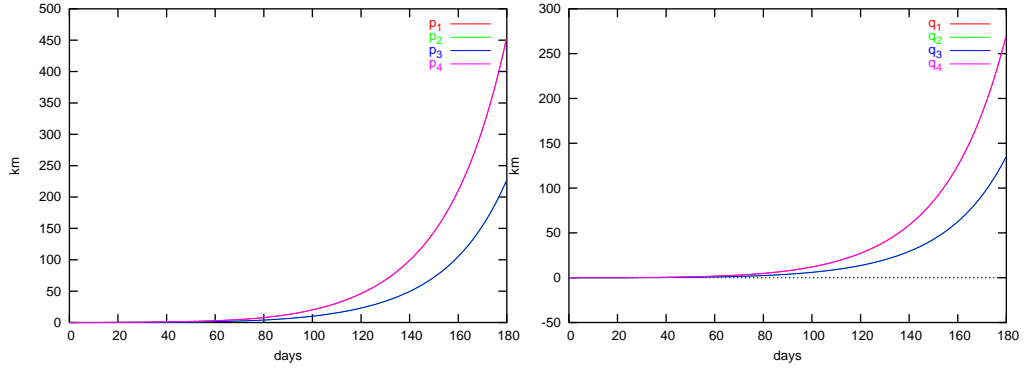


Figure 9: Deviations  $d(p_i(t), p_0(t)) - d(p_i(0), p_0(0))$  from the starting separations from the nominal orbit of the  $p_i$  points (left) and the  $q_i$  points (right) for a 180-day interval in the JPL model.

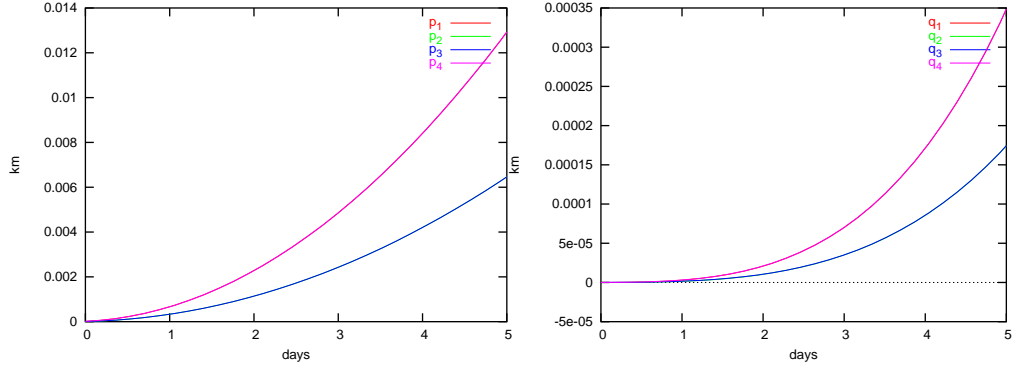


Figure 10: Deviations  $d(p_i(t), p_0(t)) - d(p_i(0), p_0(0))$  from the starting separations from the nominal orbit of the  $p_i$  points (left) and the  $q_i$  points (right) for a 5-day interval in the JPL model.

## CONTROLLED MOTIONS CONNECTING THE ZRRA CONES

In this section we will show some results related to the control of a formation moving within the zero radial acceleration cones. We have used two different control strategies: a bang-off-bang control and a minimum weighted total  $\Delta v$  consumption. For both strategies several parametric studies have been done, considering different geometrical possibilities, such as parallel and non-parallel translations between ZRRA cones.

### The bang-off-bang control

For simplicity, we will assume that the formation has only three spacecraft: two of them at the edges of a segment and the third one at the middle point. This third spacecraft will move along the reference halo orbit without any control acting on it.

The situation considered sets the formation, at the initial epoch, on a generatrix of a cone associated the reference halo orbit. As the central spacecraft moves along the orbit,



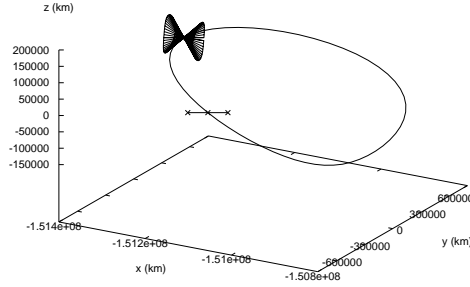


Figure 11: After some  $\Delta t$  the spacecraft are on a line parallel to the initial configuration, which is on a generatrix of a zero radial acceleration cone.

the other two are forced to be always on a segment parallel to the initial one, keeping their mutual distances fixed. This situation is illustrated in Fig. 11. We have used different values for the time displacement of the central spacecraft along the reference orbit:  $\Delta t = 2, 3, 4$  and 5 days. For any of these values, we have computed the impulsive manoeuvres that set the spacecraft at the corresponding edges of the segment in the same amount of time. It must be noted that once the formation has moved from its initial position, the segment that contains it is not, in general, on any generatrix of any zero radial acceleration cone.

If  $\mathbf{x}_i$ ,  $\mathbf{x}_f$  represent the initial and final states (position and velocity) of a spacecraft,  $\Delta \mathbf{v}_1$ ,  $\Delta \mathbf{v}_2$  the manoeuvres to be applied and  $\varphi_t$  the flow of the RTBP, the equations that must be solved for the computation of the impulsive translation manoeuvres are

$$\varphi_{(1-\alpha)\Delta t} \left[ \varphi_{\alpha\Delta t} \left( \mathbf{x}_i + \begin{pmatrix} 0 \\ \Delta \mathbf{v}_1 \end{pmatrix} \right) + \begin{pmatrix} 0 \\ \Delta \mathbf{v}_2 \end{pmatrix} \right] = \mathbf{x}_f.$$

Note that this is a system of six equations with seven unknowns: the components of the two impulses and the parameter  $\alpha$ . We have used the value of  $\alpha$  that minimises  $\|\Delta \mathbf{v}_1\| + \|\Delta \mathbf{v}_2\|$ , although there is not a significant variation of this magnitude with  $\alpha$ .

Fig. 12 shows the total cost (cm/s) for the two spacecrafts, of the parallel translation manoeuvres, for  $\Delta t = 2, 3, 4$  and 5 days, when the vertex of the departure cone moves along the halo orbit and the distance between the spacecraft at the edges of the segment is of 1 km. Only one generatrix has been taken on each cone. The  $\Delta v$  required for the manoeuvres of each spacecraft is, approximately, one half of the total cost. For any value of  $\Delta t$  there is a point on the halo orbit at which the cost of the translation is maximum. This point corresponds to the lower point of the halo orbit, which is the point at which the gravitational influence of the Earth is larger and the cost of the transfer at this (or any other) point behaves almost linearly with  $\Delta t$ .

Next we have looked for the minimum and maximum cost generatrices along the departure cone. The results are given in Fig. 13. As it is clearly seen, for any value of the  $\Delta t$  displacement, there are two angles on the cone for which the cost of the transfer is mini-

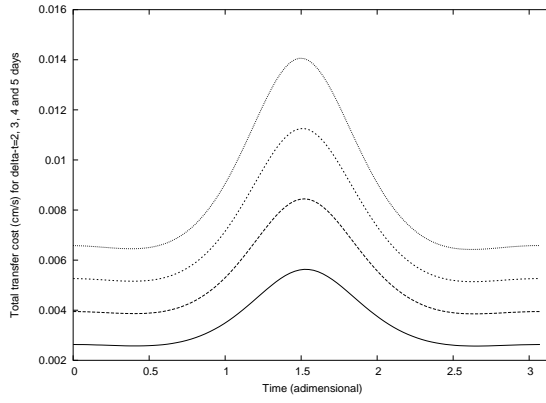


Figure 12: From bottom to top, the different curves represent the total cost (cm/s) of the parallel translation manoeuvres for  $\Delta t = 2, 3, 4$  and 5 days, when the vertex of the departure cone moves along the halo orbit. The distance between spacecraft at the edges of the segment is of 1 km. Only one generatrix has been taken on each cone.

imum and two other values for which is maximum. The angles, along the departure cone, corresponding to these four situations are, approximately, equal to  $0, \pi/2, \pi, 3\pi/2$  and  $2\pi$ . These four directions will be used later.

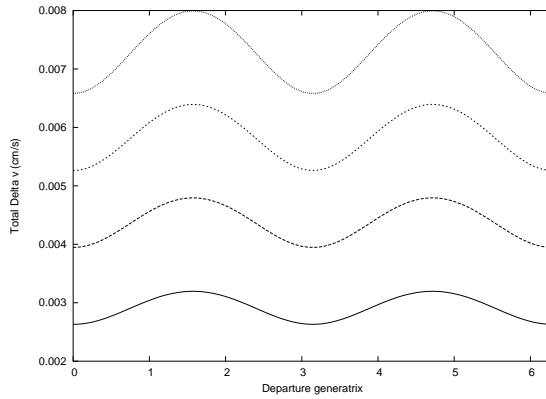


Figure 13: Behaviour of the parallel translation cost (cm/s) as a function of the angle of the generatrix on the departure cone. The curves correspond to different values of  $\Delta t = 2, 3, 4, 5$  (from bottom to top, respectively). The vertex of the cone has been kept fixed as in Fig. 11.

For the second kind of explorations, both the initial and final configurations of the formation are on a generatrix of a zero radial acceleration cone, so the transfer is non-parallel.

In the first exploration, the departure generatrix is fixed and the arrival one moves along the arrival cone, at a distance  $\Delta t$  from the first. The cones have been parametrised by an angle that varies between  $0$  and  $2\pi$ . The results corresponding to these transfers are given

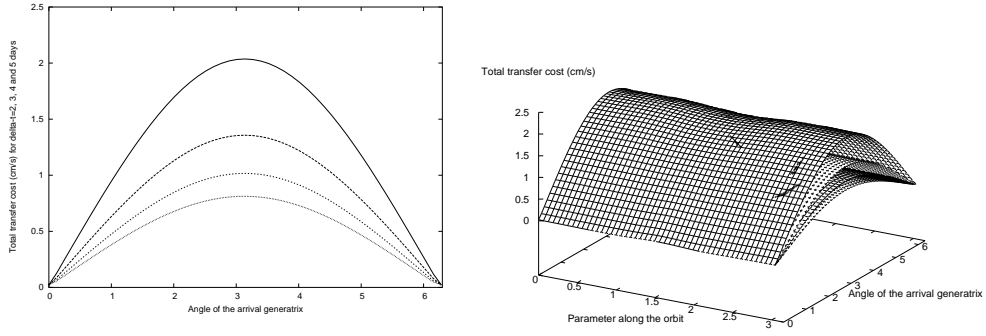


Figure 14: Total cost (cm/s) of the non-parallel translation manoeuvres between two zero radial acceleration cones separated  $\Delta t = 2, 3, 4$  and  $5$  days (top to bottom curves and surfaces). In the left figure, the departure configuration is fixed on a generatrix with angle equal to zero and the final one moves along the arrival cone, that has been parametrised by an angle varying between  $0$  and  $2\pi$  represented on the  $x$  axis of the figure. In the right hand side figure the initial point moves along the halo orbit ( $x$ -axis measured in adimensional time).

in Fig. 14. When the initial configuration is almost parallel to the final one (both with angle along the cone equal to zero) the cost of the transfer is minimum, independently of the value of  $\Delta t$ . This pattern of behaviour of the cost function is independent of the position of the initial configuration along the halo orbit, as is shown in Fig. 14 (right). From this figure one can see that the cost decreases as  $\Delta t$  increases. This is true for almost all the values of angle of the arrival generatrix except for those close to zero, for which the situation is reversed, according to Fig. 12.

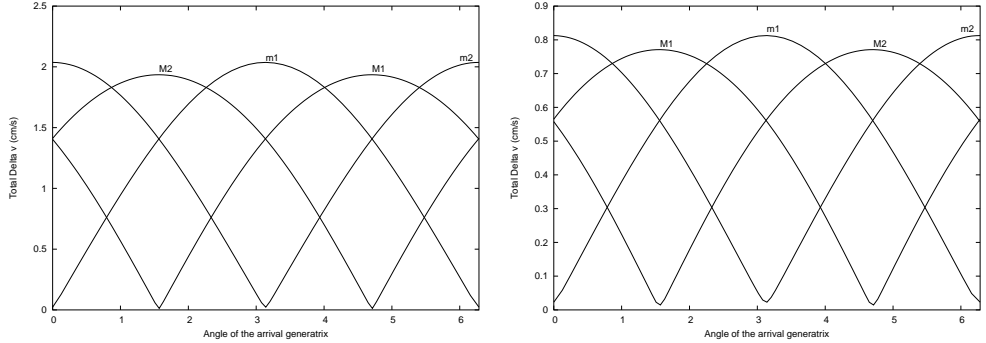


Figure 15: Total cost (cm/s) of the non-parallel transfers from the minimum (m1 and m2 curves) and maximum (M1 and M2 curves) transfer cost directions of the departure cone. The left figure corresponds to  $\Delta t = 2$  and the figure on the right to  $\Delta t = 5$  days.

Next, we have taken as departure generatrices those which correspond to the minimum and maximum values of the cost function from the parallel transfers. The results are given

in Fig. 15 for  $\Delta t = 2$  and 5 days.

Finally, we have studied the transfers from an arbitrary generatrix to an arbitrary generatrix of two fixed cones. The results are shown in Fig. 16. From this figure is clear that the cost surfaces reach their minimums on the diagonal of the  $x - y$  plane. This means that the transfer costs are minimum when both the initial and final generatrix are almost parallel.

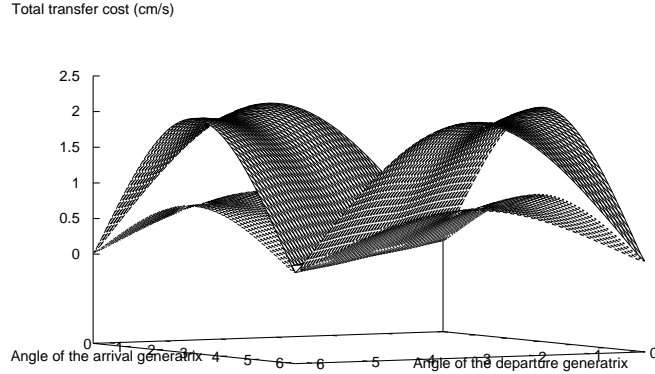


Figure 16: Total cost (cm/s) of the cone to cone transfers for  $\Delta t = 2$  (lower surface) and 5 days (upper surface) as a function of the departure and arrival angles of the generatrices on their respective cones.

### The minimum $\Delta v$ control strategy

The control procedure solves the following basic problem: consider a nominal path, defined by a certain initial state

$$(t_0, x_0, v_0),$$

and a true state of the spacecraft at  $t = t_0$ , given by (see Fig. 17)

$$(t_0, x_0 + \Delta x, v_0 + \Delta v) = (t_0, x_t, v_t).$$

The goal is to recover the nominal path at a certain epoch  $t_N > t_0$ , this is, we want to reach the state

$$\phi_{t_N - t_0}(x_0, v_0),$$

where  $\phi$  is the flow associated to the problem. The solution to this basic problem can be easily adapted in the case that the final state of the spacecraft, at  $t = t_N$ , is not  $\phi_{t_N - t_0}(x_0, v_0)$  but some well defined state:  $\phi_{t_N - t_0}(x_0, v_0) + (\Delta x_N, \Delta v_N)$ .

This control problem has been solved as follows: we introduce a sequence of manoeuvres

$$\Delta v_0, \Delta v_1, \dots, \Delta v_N,$$

to be done at some chosen epochs

$$t_0, t_1, \dots, t_N.$$

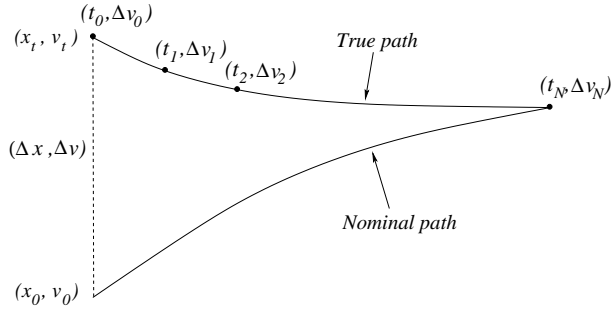


Figure 17: Illustration of the control procedure.

The manoeuvres should then verify the following constraint

$$\phi_{t_N-t_{N-1}} (\dots \phi_{t_2-t_1} (\phi_{t_1-t_0}(x_t, v_t + \Delta v_0) + \Delta v_1) + \dots + \Delta v_{N-1}) + \Delta v_N = \phi_{t_N-t_0}(x_0, v_0).$$

Of course, there are infinitely many different values of  $\Delta v_0, \Delta v_1, \dots, \Delta v_N$  verifying the above equation. The ones selected minimise

$$\sum_{j=0}^N q_j \|\Delta v_j\|^2,$$

where  $q_0, \dots, q_N$  are weights which must be fixed in advance. For the simulations we have used

$$q_j = 2^{-j},$$

so the magnitude of two consecutive manoeuvres decays approximately by a factor of 2. For the solution of this problem, the flow  $\phi$  can be replaced by its linear approximation, given by the variational equations, provided we are not far from the nominal path.

The basic parameters of the control procedure are:

*The tracking time interval:  $T_t$ .* Every  $T_t$  time units the formation is tracked and a control manoeuvre is started. Each control manoeuvre is composed by several correction manoeuvres. At the end of a tracking time interval all the correction manoeuvres, of a certain control manoeuvre, must be finished.

*The time interval for the execution of manoeuvres:  $T_m (= t_N - t_0)$ .* Is the time required by the spacecrafts to recover the formation. It must be such that  $T_m \leq T_t$ . In the simulation program, during this time interval all the correction manoeuvres are executed at uniformly distributed instants ( $t_{i+1} - t_i = \text{constant}$ ). This choice can be easily modified.

*The number of correction manoeuvres of each control:  $N$ .* In order that each spacecraft can recover its position in the formation, at least two correction manoeuvres must be done

(assuming that they are performed without errors). We have foreseen the execution of  $N \geq 2$  correction manoeuvres with decreasing magnitude (the decay will be approximately as  $1/2^n$ ). A typical plot displaying this kind of behaviour, for the magnitude of the correction manoeuvres as a function of time, is shown in Fig. 18.

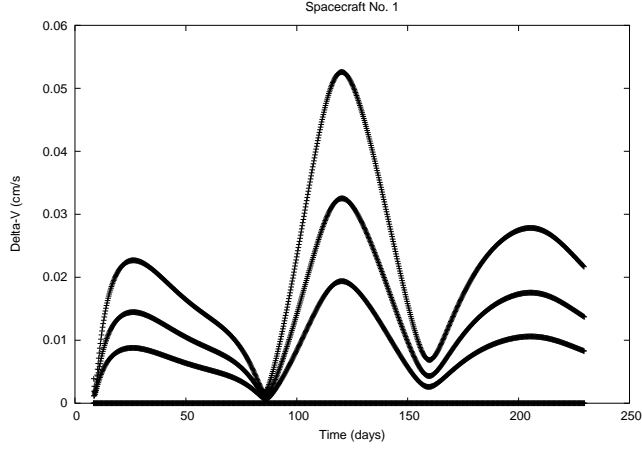


Figure 18: Magnitude of the correction manoeuvres as a function of time. Each control manoeuvre is composed by 4 correction manoeuvres with decreasing magnitude.

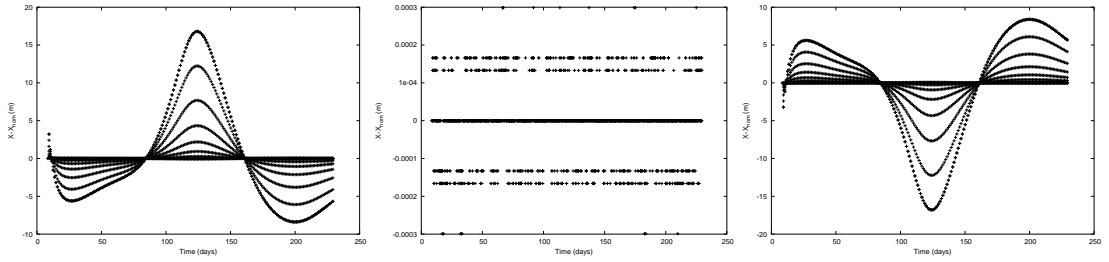
## SIMULATION PARAMETERS AND SUMMARY OF RESULTS

We have done several simulations in order to see the behaviour of the formation using different sets of values of the free parameters, according to the following table.

Angle $\alpha_0$	Distance $d_1$	Distance $d_2$	Tracking interval	Number of manoeuvres	Execution time interval
Fixed	Fixed	Fixed	<b>Free</b>	Fixed	Fixed
Fixed	Fixed	Fixed	Fixed	Fixed	<b>Free</b>
Fixed	Fixed	Fixed	Fixed	<b>Free</b>	Fixed
Fixed	<b>Free</b>	<b>Free</b>	Fixed	Fixed	Fixed
<b>Free</b>	Fixed	Fixed	Fixed	Fixed	Fixed

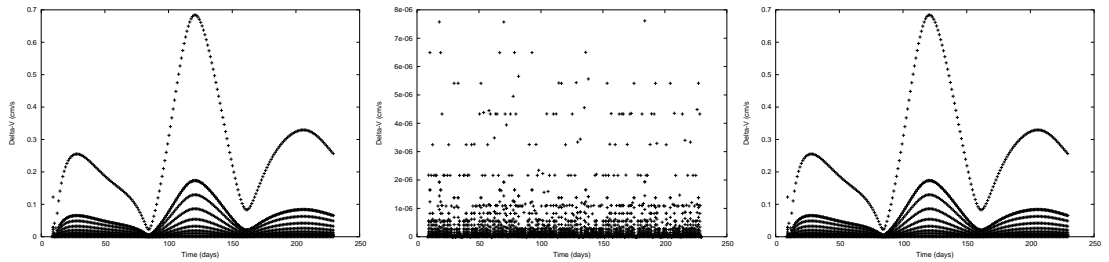
For a given set of values of the parameters we have analysed the behaviour of several variables:

1. For each spacecraft of the formation, the  $x$ ,  $y$  and  $z$  components of the differences between the actual position of the spacecraft and its nominal one. These differences are shown as a function of time. A typical result, for the  $x$  component, is displayed in the following figure:

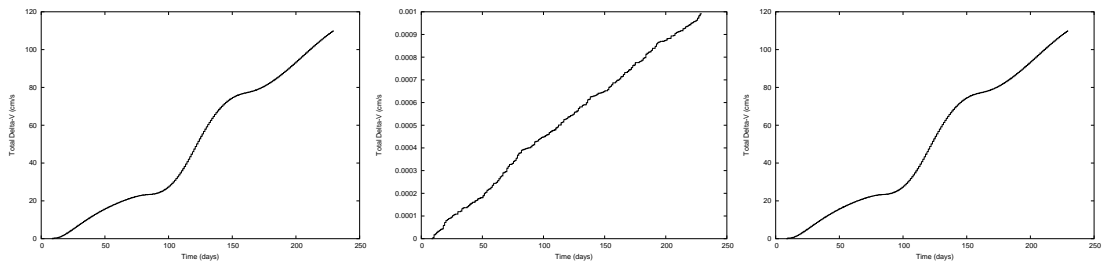


Each column corresponds to a different spacecraft. Since, for this simulation, the two edge spacecrafts of the formation are at the same distance from the central one, their corresponding figures are almost symmetrical. The deviation of the central spacecraft with respect to its nominal position is almost negligible, since we require for this s/c to follow a true trajectory of the model problem (the RTBP). Each time a correction manoeuvre is applied, the deviation decreases and it is almost zero after the last correction manoeuvre of a given control manoeuvre.

- For each spacecraft of the formation, the magnitude of the control manoeuvres applied. An example is shown in the next figure. Of course, the magnitude of the controls are closely related to the deviations, so the pattern of these figures is close the previous ones.



- For each spacecraft of the formation, the total magnitude of the controls applied (which is the sum of the magnitudes of all the control manoeuvres). The following figure is an example.



The following items summarise the basic results obtained:

1. The best results are obtained for a spacecraft at  $d = 0.5$  km, with a tracking time interval equal to the execution of manoeuvres time interval:  $T_t = T_M = 5$  hours. During this interval  $N = 5$  manoeuvres are executed. The total  $\Delta v$  required for the transfer of this spacecraft, keeping its formation configuration, is approximately equal to 14.2 cm/s.
2. In the above case, if the distance  $d$  is doubled, the total  $\Delta v$  is also multiplied by 2.
3. For the simulations done varying the tracking time interval and keeping fixed the remaining parameters it has been found that:
  - (a) The maximum deviation increases almost linearly with the tracking interval.
  - (b) The maximum  $\Delta v$  increases also almost linearly with the tracking interval.
  - (c) For a large set of values of the tracking interval, The total  $\Delta v$  is almost constant. When the tracking interval is less than 4 hours, the  $\Delta v$  decreases abruptly and can be reduced even to a 70% of its almost constant value.
4. For the simulations done varying the execution of manoeuvres time interval and keeping fixed the remaining parameters it has been found that:
  - (a) The maximum deviations seem to be independent of the free parameter and remain almost constant.
  - (b) There is an almost exponential decrease of both the maximum and the total  $\Delta v$  when the time interval for the execution of manoeuvres increases and gets close to the length of the tracking interval.
5. For the simulations done varying the number of manoeuvres it has been found that:
  - (a) The maximum deviations seem to be independent of the free parameter and remain almost constant.
  - (b) Both, the maximum and the total  $\Delta v$  increase almost linearly with the number of manoeuvres. The best values are obtained when only two manoeuvres are executed.
6. For the simulations done varying the separation between the spacecrafts it has been found that:
  - (a) When the separation increases, the maximum deviations do also in an almost linear way. This is true up to separations of the order of 3 km, which probably are at the boundary of the linear approximations used.
  - (b) Both, the maximum and the total  $\Delta v$  increase almost linearly with the separation between the spacecrafts. The best values are obtained when i this separation is very small.



7. For the simulations done varying the angle  $\alpha_0$  in the cone of zero relative radial accelerations, it has been found that:
- (a) The smallest deviations are found for values of the angle between 60 and 120 degrees.
  - (b) Close to  $\alpha_0 = 60^\circ$  and  $\alpha_0 = 300^\circ$  there are two local minima of the total  $\Delta v$ .

## CONCLUSIONS

In this paper we have introduced some new manifolds associated to any natural trajectory suitable for formation flight. The natural motion, using initial conditions for the spacecraft of the formation on these manifolds, avoids large variations of the mutual distances between the spacecraft. Different kinds of controlled motions between these manifolds have been analysed.

## ACKNOWLEDGEMENTS

This work is part of the DICOFF project done in collaboration with Deimos Space S.L. and has been partially supported by the grant PNE-010/2002-I-A of the Spanish Programa Nacional del Espacio.

The authors have been also partially supported by grants CIRIT 2001SGR-70, 2003XT-00021 (Catalonia) and grant BFM2003-09504 (MCYT, Spain). M. Marcote acknowledges the support of the doctoral research grant AP2001-3064 (MECD, Spain)

## References

- [1] G. Gómez, M.W. Lo, and J.J. Masdemont (Eds.) “Libration Point Orbits and Applications” *World Scientific*, 2003.
- [2] V. Szebehely. *Theory of Orbits*. Academic Press, 1967.